

Article

Reverse Chemical Proteomics Identifies an Unanticipated Human Target of the Antimalarial Artesunate

Michael P. Gotsbacher, Sungmin Cho, Nam Hee Kim, Fei Liu, Ho Jeong Kwon, and Peter Karuso

ACS Chem. Biol., **Just Accepted Manuscript** • DOI: 10.1021/acscchembio.8b01004 • Publication Date (Web): 06 Mar 2019

Downloaded from <http://pubs.acs.org> on March 7, 2019

Just Accepted

“Just Accepted” manuscripts have been peer-reviewed and accepted for publication. They are posted online prior to technical editing, formatting for publication and author proofing. The American Chemical Society provides “Just Accepted” as a service to the research community to expedite the dissemination of scientific material as soon as possible after acceptance. “Just Accepted” manuscripts appear in full in PDF format accompanied by an HTML abstract. “Just Accepted” manuscripts have been fully peer reviewed, but should not be considered the official version of record. They are citable by the Digital Object Identifier (DOI®). “Just Accepted” is an optional service offered to authors. Therefore, the “Just Accepted” Web site may not include all articles that will be published in the journal. After a manuscript is technically edited and formatted, it will be removed from the “Just Accepted” Web site and published as an ASAP article. Note that technical editing may introduce minor changes to the manuscript text and/or graphics which could affect content, and all legal disclaimers and ethical guidelines that apply to the journal pertain. ACS cannot be held responsible for errors or consequences arising from the use of information contained in these “Just Accepted” manuscripts.



ACS Publications

is published by the American Chemical Society, 1155 Sixteenth Street N.W., Washington, DC 20036

Published by American Chemical Society. Copyright © American Chemical Society. However, no copyright claim is made to original U.S. Government works, or works produced by employees of any Commonwealth realm Crown government in the course of their duties.

Reverse Chemical Proteomics Identifies an Unanticipated Human Target of the Antimalarial Artesunate

Michael P. Gotsbacher,^{1†} Sungmin Cho,^{2‡} Nam Hee Kim,² Fei Liu,¹ Ho Jeong Kwon,^{2*} and Peter Karuso^{1*}

¹Department of Molecular Sciences, Macquarie University, Sydney, NSW 2109, Australia.

²Chemical Genomics Global Research Laboratory, Department of Biotechnology, College of Life Science & Biotechnology, Yonsei University, 50 Yonsei-ro, Seodaemun-gu, Seoul 120-749

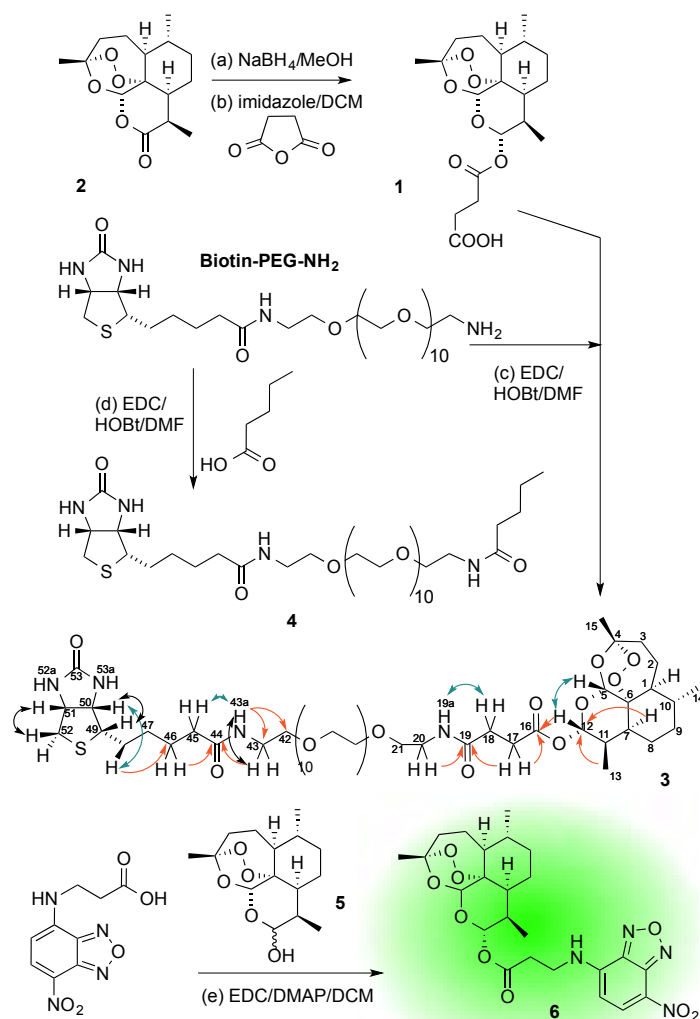
ABSTRACT: Artemisinins are the most potent and safe antimalarials available. Despite their clinical potential, no human target for the artemisinins is known. The unbiased interrogation of several human cDNA libraries, displayed on bacteriophage T7, revealed a single human target of artesunate; the intrinsically disordered Bcl-2 antagonist of cell death promoter (BAD). We show that artesunate inhibits the phosphorylation of BAD, thereby promoting the formation of the proapoptotic BAD/Bcl-xL complex and the subsequent intrinsic apoptotic cascade involving cytochrome c release, PARP cleavage, caspase activation and ultimately cell death. This unanticipated role of BAD as a possible drug target of artesunate points to direct clinical exploitation of artemisinins in the Bcl-xL life/death switch and that artesunate's anticancer activity is, at least in part, independent of reactive oxygen species.

The study of weak, but selective, protein–ligand interactions has always been a challenge and is exemplified by gamma-hydroxybutyric acid, which is a 3 mM agonist of GABA-B receptors but highly selective.¹ Low affinity effectively hinders the identification of small molecule protein targets using genome-wide, forward proteomic methods such as affinity capture MS or affinity chromatography.² Even high affinity interactions can be problematic to identify in the presence of large amounts of non-specific interactions. An attractive alternative approach, particularly suited for weak interactions with low abundance proteins, is reverse chemical proteomics using phage display where there is a physical link between the genome and proteome.^{3–13} The rapid life cycle of bacteriophages allows iterative purification of rare and/or low abundance proteins from highly complex mixtures based on relatively weak affinity to a tagged small molecule. For example, we were able to rapidly isolate a human protein target for kahalalide F that showed ~50 μ M K_D with ribosomal protein S25.⁹ Here we report the identification of the Bcl-2 agonist of cell death (BAD) promoter as the first human target of the natural product drug artesunate (**1**) using T7 phage display.

Artemisinins are sesquiterpenes from the sweet wormwood (*Artemisia annua*).^{14, 15} They are the most potent antimalarials available with 500 million doses/annum prescribed to eradicate *Plasmodium falciparum* infections¹⁶ but their mode of action is still under debate.¹⁷ It is however widely accepted that inside

the infected red blood cell, the endoperoxide bridge of artemisinin is activated and cleaved through a heme-dependent, radical mechanism that alkylates parasite proteins.^{18–20} This has recently been supported through chemical proteomics investigations in which at least 124 parasite proteins were shown to be alkylated by an artesunate analogue in infected red blood cells.²¹ Notwithstanding this, proposed specific targets include SERCA,²² membrane glutathione S-transferase (PfEXP1)²³ or phosphatidylinositol-3-kinase PfPI3K in *P. falciparum*.²⁴

Scheme 1. Synthesis^a of probes and NMR correlations for probe **3**; red = HMBC, green = ROESY, black = COSY, showing key correlations only.



^a Reagents and conditions: (a) **2**, NaBH_4 (3.5 equiv)/MeOH, 0–5 °C, 2 h, 81% yield; (b) **5**, succinic anhydride (1.6 equiv), imidazole (0.9 equiv)/DCM, rt 2 h, 91% yield; (c) Biotin-PEG-NH₂, **1** (2 equiv), EDC (4 equiv), HOBt (4 equiv)/DMF, 0 °C over 30 min, then rt 18 h, then excess water, 39% yield; (d) Biotin-PEG-NH₂, valeric acid (2 equiv), EDC (3 equiv), HOBt (3 equiv)/DMF, 0 °C over 30 min, then rt 18 h, then excess water, 28% yield; (e) NBD-Cl (1.2 equiv)/ACN, β -alanine (1.2 equiv) and NaHCO₃ (3 equiv)/water, 55 °C, 1 h; then remove ACN, pH to 2 (1 N HCl); solvent removal, then **5** (1 equiv)/DCM, DMAP (1.2 equiv) under N₂; then EDC (1.2 equiv), rt 18 h, 42% yield over two steps.

Interestingly, artemisinins display polypharmacology, with profound and selective anticancer activity^{25, 26} and, it has been suggested, promote apoptosis via mitochondrial pathways in cancer cell lines.^{27–29} It is known that many genes are upregulated upon **1** treatment in cancer cell lines. These include BUB3, cyclins, CDC25A (proliferation), VEGF, MMP-9, angiostatin, thrombospondin-1 (angiogenesis), and Bcl-2, BAX, NF- κ B (apoptosis).^{27, 30} Despite their clinical potential for treating cancer and the

extensive primary literature on their anticancer activity, **1**'s human target remains elusive.^{31–34}

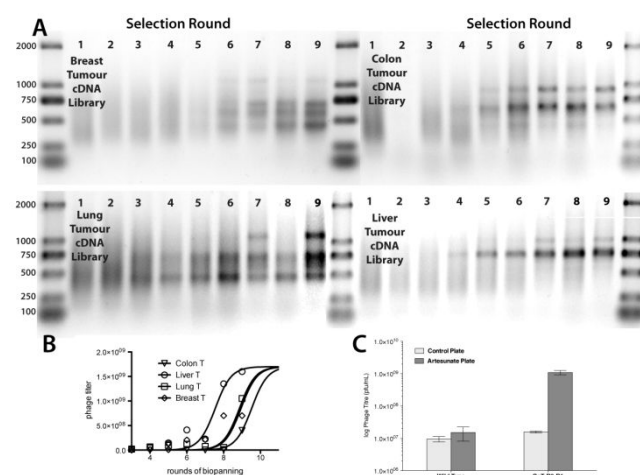


Figure 1. BAD is the common protein binding partner of **1**, identified by biopanning of phage displayed cDNA libraries from various cancer cells. (A) Agarose gel electrophoresis of phage DNA inserts, amplified by PCR from phage sub-libraries after biopanning against **5** immobilized on neutravidin-coated microtiter plates. See Figures S4 and S5 for more detail. (B) Phage titer after each round of biopanning showing convergence after rounds 8–10 for the 4 tumor cDNA libraries and (C) On-phage binding study showing 100-fold higher titer of the BAD-displaying phage clone for the **1**-immobilized support than the support with immobilized negative control (**4**). The wild-type phage (no insert) does not differentiate the two supports.

RESULTS AND DISCUSSION

We began with the synthesis of a biotinylated analog (**3**) of **1** from artemisinin (**2**) containing a long, hydrophilic linker (Biotin-PEG-NH₂; Scheme 1). Derivatization at C12 is known to not affect the anticancer activity of artemisinins.³⁵ The structure, purity, stereochemistry and stability were verified by HPLC, NMR spectroscopy and HRMS (Scheme 1; Figures S1–S2). Likewise, a biotinylated “blank probe” reagent (**4**) was synthesized from valeric acid, along with **6**, a fluorescent analog of **1** for imaging (F-ART, Scheme 1; Figure S3). Compound **3** and **4** were immobilized in separate neutravidin coated microtiter strip wells. Five human cDNA libraries, expressed in bacteriophage T7, were panned against **3** coated wells, after preclearing in **4** wells to remove non-specific binders. After 9 rounds of biopanning, all four tumor libraries produced dominant clones but the normal colon library did not converge (Figure 1A; Figure S4). For all four tumor libraries, the phage titer increased exponentially after round 8 (e.g. Figure 1C). Random plaques were picked after the last round and fingerprinted by *Hinf*I digestion (Figure S5). From sequencing, in all converged tumor libraries, the dominant clone (Table S4) was the Bcl-2 antagonist of cell death promoter (BAD). Comparison of the DNA sequences

showed that for each library the phage selection produced BAD clones of different lengths, but all were in-frame with the phage coat protein and covered the full coding sequence of BAD (Table 1). No other gene was represented by in-frame clones that appeared in more than one tumor library.

Table 1. Sequence alignment of BAD clones from colon tumor (CoT), liver tumor (LiT), lung tumor (LuT) and breast tumor (BrT) cDNA phage libraries and consensus with human BAD^a.

		-10	0 ^b	10	20	30
CoT_B1SDRAWAQ	MFQIPEFEP	EQEDSSSAER	GLGSPAGDG	
LiT_C6GAWAQ	MFQIPEFEP	EQEDSSSAER	GLGSPAGDG	
LuT_B7SRDRAWAQ	MFQIPEFEP	EQEDSSSAER	GLGSPAGDG	
LuT_G9GAWAQ	MFQIPEFEP	EQEDSSSAER	GLGSPAGDG	
BrT_C10	REAAAGPGQ	GPRDRAWAQ	MFQIPEFEP	EQEDSSSAER	GLGSPAGDG	
BADrdrAWAQ	MFQIPEFEP	EQEDSSSAER	GLGSPAGDG	
ConsensusrdrAWAQ	MFQIPEFEP	EQEDSSSAER	GLGSPAGDG	

		40	50	60	70	80
CoT_B1	PSGSGKHHRQ	APGLLDASH	QEQPTSSSH	HGGAGAVEIR	SRHSSYPAGT
LiT_C6	PSGSGKHHRQ	APGLLDASH	QEQPTSSSH	HGGAGAVEIR	SRHSSYPAGT
LuT_B7	PSGSGKHHRQ	APGLLDASH	QEQPTSSSH	HGGAGAVEIR	SRHSSYPAGT
LuT_G9	PSGSGKHHRQ	APGLLDASH	QEQPTSSSH	HGGAGAVEIR	SRHSSYPAGT
BrT_C10	PSGSGKHHRQ	APGLLDASH	QEQPTSSSH	HGGAGAVEIR	SRHSSYPAGT
BAD	PSGSGKHHRQ	APGLLDASH	QEQPTSSSH	HGGAGAVEIR	SRHSSYPAGT
Consensus	PSGSGKHHRQ	APGLLDASH	QEQPTSSSH	HGGAGAVEIR	SRHSSYPAGT

		90	100	110	120	130
CoT_B1	EDDEGMGEEP	SPFRGRSRA	PPNLWAAQRY	GRELRMSDE	FVDSFKKGLP
LiT_C6	EDDEGMGEEP	SPFRGRSRA	PPNLWAAQRY	GRELRMSDE	FVDSFKKGLP
LuT_B7	EDDEGMGEEP	SPFRGRSRA	PPNLWAAQRY	GRELRMSDE	FVDSFKKGLP
LuT_G9	EDDEGMGEEP	SPFRGRSRA	PPNLWAAQRY	GRELRMSDE	FVDSFKKGLP
BrT_C10	EDDEGMGEEP	SPFRGRSRA	PPNLWAAQRY	GRELRMSDE	FVDSFKKGLP
BAD	EDDEGMGEEP	SPFRGRSRA	PPNLWAAQRY	GRELRMSDE	FVDSFKKGLP
Consensus	EDDEGMGEEP	SPFRGRSRA	PPNLWAAQRY	GRELRMSDE	FVDSFKKGLP

		140	150	160
CoT_B1	RPKSAGTATQ	MRQSSSWTRV	FQSWWDRNLG	RGSSAPSQ
LiT_C6	RPKSAGTATQ	MRQSSSWTRV	FQSWWDRNLG	RGSSAPSQ
LuT_B7	RPKSAGTATQ	MRQSSSWTRV	FQSWWDRNLG	RGSSAPSQ
LuT_G9	RPKSAGTATQ	MRQSSSWTRV	FQSWWDRNLG	RGSSAPSQ
BrT_C10	RPKSAGTATQ	MRQSSSWTRV	FQSWWDRNLG	RGSSAPSQ
BAD	RPKSAGTATQ	MRQSSSWTRV	FQSWWDRNLG	RGSSAPSQ

^a The BH3 domain of BAD is highlighted in blue and the phosphorylated Ser residues in green. Each library converged on full-length BAD with many different clones varying in N- and C-terminal sequences but all were in-frame with the coat protein. The **bolded/underlined** residues are the consensus binding domains from the peptide dot blot experiments (see Table S5, Figures S13–S14).

^b The mouse numbering system is widely used in the literature and is 36 amino acids longer than human BAD. Thus S99 above is S136 in the mouse sequence and to avoid confusion the mouse numbering is used throughout.

Several attempts to clone and overexpress BAD as hexaHis or GST fusions failed due to the intrinsic disorder of the BAD protein.³⁶ Attempted purification led to extensive degradation so it was not possible to obtain a pure sample for reliable K_D measurements. Consequently, an on-phage binding assay (Figure 1C) was used and showed that the control phage (no insert) produced a background of $\sim 10^7$ phage particles upon elution with SDS in wells derivatized with **3** or **4**. In contrast, BAD-phage (with BAD insert)

produced $100\times$ more phage particles upon elution from **3** derivatized wells compared to **4**, suggesting a specific interaction between BAD and **1**. As an alternative to quantitative K_D measurements, we constructed a peptide library of BAD peptides (31×20 -mers shifted by 5 aa each time; Table S5) arrayed onto a glass slide. Staining with **6**, with butylamine-NBD as a negative control (Figure S13), indicated preferential binding of **6** to a section around S136, just before the BH3 domain, and to the C-terminal of the protein (Figure S14).

BAD, as a BH3-only, proapoptotic protein, was originally identified as a partner for Bcl-2 and Bcl-xL in a yeast 2-hybrid screen and shown to displace BAX to induce cytochrome c release and caspase-dependent apoptosis.³⁷ To validate the dependence of **1**'s apoptotic activity on BAD, cell proliferation assays were performed first using HeLa (human cervical cancer) cells (Figure S6.), providing LD₅₀ values of 63, 38 and 12 μM ($R^2 = 0.94\text{--}0.98$) for 24, 48 and 72 h **1** treatments, respectively, and established upper limits on the concentrations of **1** that can be used in live cells. The apoptotic effect of **1** was also confirmed in HeLa cells by observation of a dose dependent release of cytochrome c into the cytosol, PARP cleavage and caspase activation (Figures S7–S9). Under the microscope, cells treated with $\geq 10\text{ }\mu\text{M}$ **1** showed typical signs of apoptosis (Figure S12).

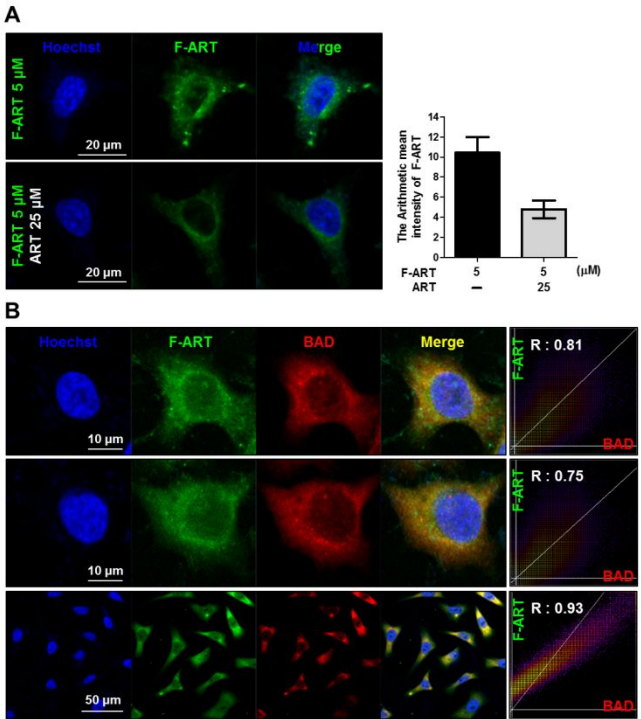


Figure 2. Validation of the interaction between **1** and BAD using fluorescently labeled **1** (F-ART, **6**). (A) Competition between **1** (ART) and **6** (F-ART). Panel 1: Treatment of HeLa cells with Hoechst (blue) and **6** (green). Panel 2: Treatment of HeLa cells with Hoechst (blue) and **6** (green) in the presence of 25 μM **1**. The intensity of **6** was measured using Image J

and displayed as a bar graph. (B) Co-localization of **6** (green) and BAD-Ab (red). Panel 1, 2: Treatment of HeLa cells with Hoechst (blue) and 10 μM **6** (green) and BAD-Ab (red). Panel 3: showing additional cells. The colocalization of F-ART and BAD was measured using Image J and expressed as a Pearson correlation curve.

The binding of ART to BAD was further investigated in HeLa cells through confocal microscopy. In order to investigate the binding of ART to BAD in living cells, F-ART (**6**) was synthesized and used in a competitive binding assay. Cells that were pretreated with unlabeled ART (**1**) and then stained with **6** (Fig. 2A, panel 2), showing a 60% reduction in fluorescence, demonstrating that **6** and **1** share the same binding site in the cytosol of HeLa cells (Figure 2A). BAD and **6** were also found to partially colocalize in the cytosol of HeLa cells (Figure 2B) and there is a positive correlation ($r^2 > 0.75$) between the localization of **6** and BAD, suggesting that **6** and **1** bind to BAD in living cells. Similar results were obtained for HEK293 cells (Figure S12). A DARTS assay with HEK293 cell lysates (Figure 3), in which the binding of a ligand to a protein is detected by either the enhanced or reduced rate of proteolysis,³⁸ suggested the binding of **1** to BAD. The proteolysis of BAD, BAX, and actin in the cell lysate was monitored in the presence of increasing pronase (0 to 10 $\mu\text{g mL}^{-1}$) and **1** (0 to 400 μM) concentrations, following the literature recommendations to apply 10 \times higher ligand concentrations as the upper limit compared to the effective concentration.³⁸ For actin (Figure 3D) and BAX (Figure 3C), hydrolysis proceeded in a **1**-independent manner. In contrast, BAD was more readily proteolyzed in a clear dose-dependent manner (Figure 3B; $p = 0.0063$), suggesting that **1** selectively binds to BAD, but not the related BAX protein or the actin loading control.

The proapoptotic action of **1** was abrogated when BAD expression was knocked down using a mixture of 4 siRNAs against BAD (siBAD) (Figure 4). In the presence of 20 nM siBAD, BAD expression in HeLa cells was reduced by ~60% compared to random siRNA (Figure 4A and 4B). Compound **1**'s apoptotic effect increased in a time and dose dependent manner (Figure 4C) that was only slightly affected by the introduction of a mixture of random siRNA (Figure 4D). In cells treated with siBAD with 40 μM **1**, the suppression of **1**'s apoptotic effect was significant (87% cells surviving with BAD knock-down vs. 65% without; Figure 4E). The loss of **1**'s apoptotic effect with 20 nM siBAD was most prominent after 72 hours of growth (71% surviving with BAD knock-down vs 20% without; Figure 4E). The same effect was observed for all concentrations of **1** tested again in a dose-dependent manner ($p = 0.055$). In contrast, the apoptotic effect of camptothecin was not responsive to changes of BAD expression (Figure S11C) because camptothecin induces apoptosis by targeting topoisomerase I.³⁹

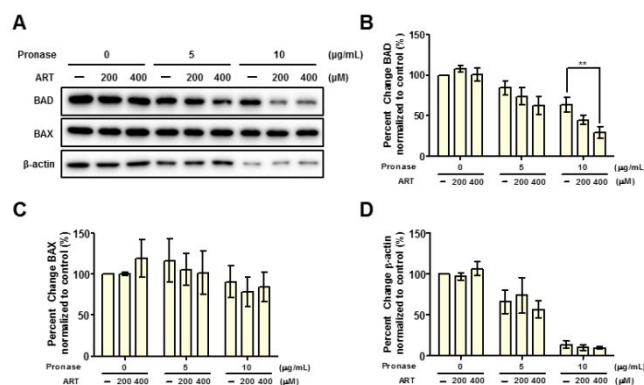


Figure 3. Validation of the interaction between **1** and BAD using the DARTS assay. (A) Western blotting of BAD, BAX and actin (loading control) with variable **1** and pronase. (B)-(D) graphical representation of (B) for BAD ($p = 0.00152$; one-way ANOVA), BAX ($p = 0.8968$) and actin ($p = 0.6592$), respectively, run in triplicate. ** Designates $p < 0.01$ (Students t -test).

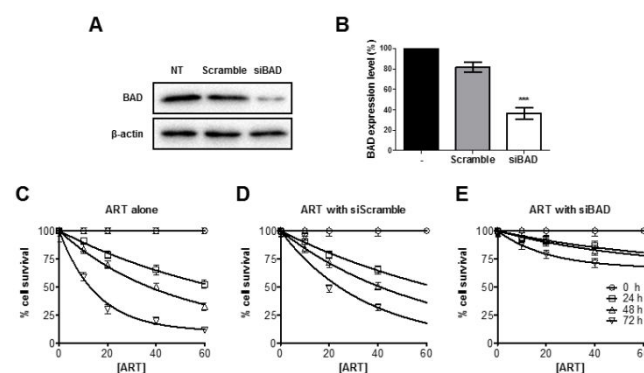


Figure 4. Validation of the interaction between **1** and BAD using siRNA. (A) BAD can be knocked down in live HeLa cells with 20 nM mixture of 4 siRNAs for BAD (lane 3) relative to random mixed siRNA (lane 2). (B) Graphical representation of (A) carried out in triplicate. (C) Percentage (relative to control) cell survival of HeLa cells treated with variable **1** for 2472 h. (D) Same as B except HeLa cells were also treated with a 20 nM mixture of random siRNA. (E) The same as (D) except cells were treated with 20 nM siRNA against BAD. *** Designates $p < 0.001$ (Students t -test).

The identification of BAD as a target of **1**'s apoptotic effect came as a surprise. Many mechanisms for the anticancer activity of artemisinins have been proposed with reactive oxygen species (ROS) generation or mitochondrial induced apoptosis, involving Bcl-2 family genes, particularly prominent in the literature.^{33, 40, 41} A cell line-dependent effect of **1** (or its various derivatives) has been reported but no target was identified.⁴² More recently, Button *et al.* argued that necroptosis is **1**'s main mode of action on Schwannoma cells.⁴³ Even more recently, Hamacher suggests "ferroptosis" in pancreatic cancer cells and that **1** did not induce apoptosis or necroptosis.⁴⁴ A recent chemical proteomics study in this journal suggested that due to heme activation, **1** covalently modified many

proteins (in HeLa cell lysates treated with 10 μ M hemin) to achieve its anticancer activity in parallel to its antimalarial activity.⁴⁵ However, this is not consistent with other studies that discount oxidative damage as necessary for cytotoxicity of **1** and demonstrate **1**-induced apoptosis in a ROS-independent, Bax-mediated manner.⁴⁶ The use of a cell lysate with a high concentration of added hemin is also not physiologically relevant. The endoperoxide of ART is known to react with free hemin.⁴⁷ Our identification of BAD as a target of **1** opens new questions in ROS-independent apoptosis and potential avenues for targeted therapies. Given that Bcl-2/Mcl-1 family members is an emerging strategy in development of anticancer therapeutics⁴⁸ and these life/death switches have been suggested as the Achilles' heel of many tumors,⁴⁹ a BAD-targeted mechanism of action for **1** in a specific apoptotic pathway could lead to synergy with other anticancer therapies.⁵⁰

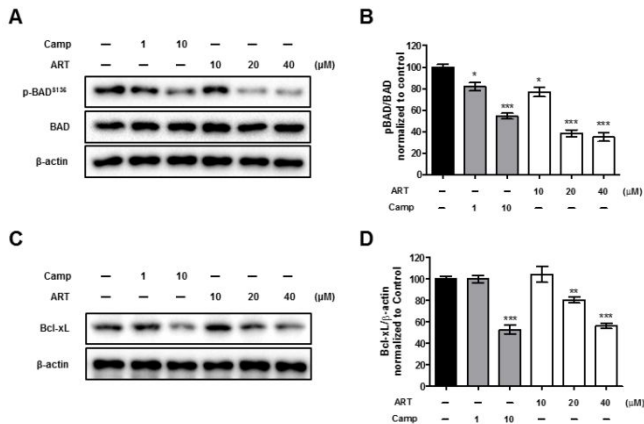


Figure 5. **1** reduces the level of S136 phosphorylation on BAD and Bcl-xL expression levels in HeLa cells. (A) Dose-dependent reduction in S136 phosphorylation on BAD in HeLa cells on treatment with **1**. (B) Graphical representation of (A) carried out in triplicate. (C) Dose-dependent reduction of Bcl-xL expression levels upon **1** treatment. (D) Graphical representation of (C) carried out in triplicate. * Designates $p < 0.05$, ** designates $p < 0.01$, *** designates $p < 0.001$ (Students t -test).

BAD can reverse the pro-survival activity of Bcl-xL, but not that of Bcl-2. Also, in rat ovaries, mutation of BAD_{S136A} results in the reported binding of BAD to Mcl-1 whereas wild-type phosphorylated BAD binds exclusively to 14-3-3.⁵¹ Regulation of BAD is achieved by cytokine and growth factor signaling and likely influences numerous aspects of metabolism, autophagy, and apoptosis.^{48, 52} In a breast cancer model where PTEN is mutated, BAD is constitutively phosphorylated and sequestered by 14-3-3, completely inhibiting its proapoptotic activity.⁵³ In AML, it was found that BAD was phosphorylated at S112 and S136 in 41/42 clinical samples tested.⁵⁴ BAD's sensitizer activity toward apoptosis is negatively regulated by kinases (JNK, PKA and AKT) through phosphorylation at S112, S136 and S155.⁵⁵⁻⁵⁷ It has been suggested the phosphorylation within the BH3

domain (S155; Table 1) renders the binding of BAD to the hydrophobic BH3 binding domain of Bcl-xL unfavorable resulting in inhibition of BAD's proapoptotic function.⁵⁸ The level of S136-pBAD was therefore measured in HeLa cells 24 h after treating with **1** (0–40 μ M) or camptothecin (positive control; 1–10 μ M) (Figure 5A). A dose dependent decrease in phosphorylation on S136 was observed (Figure 5B) with **1**, consistent with the peptide array data (Figures S13–S14). There was also a dose dependent decrease in the expression levels of Bcl-xL (Figure 5C, 5D). At 20 μ M, BAD phosphorylation was reduced by 60% and Bcl-xL by 20% respectively.

The effect of fixed doses of **1** on HeLa cells in the presence of 0, 0.01, 0.1, 1 or 10 μ M ABT-737 or camptothecin was subject to isobolographic analysis (Figure 6) to determine if **1** would work synergistically or additively with ABT-737, a clinically useful, known BH3-mimic that binds Bcl-xL.⁵⁹ HeLa cells were grown for 24 or 48 hours after treatment and the LD₅₀ determined in the presence or absence of **1** (Figure S15). As expected, **1** and camptothecin are synergistic (Figure 6B) as they target orthogonal pathways but surprisingly **1** and ABT-737 Camptothecin were also found to be highly synergistic (Figure 6A), even though BAD and ABT-737 both putatively bind Bcl-xL to achieve their apoptotic effect.

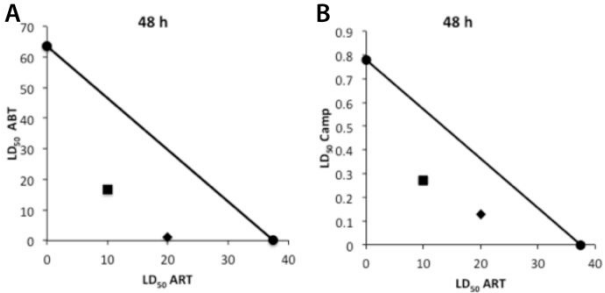


Figure 6. **1** is synergistic with ABT-737 and camptothecin. (A) Isobole analysis (from Figure S15A-C) of the interaction between **1** and ABT-737 shows a strong synergistic effect at 10 μ M (square) and 20 μ M (diamond) **1**. (B) Isobole analysis (from Figure S15d-f) of the interaction between **1** and camptothecin also shows a synergistic effect at 10 μ M (square) and 20 μ M (diamond).

As the apparent cytotoxicity of **1** is abrogated if BAD is knocked down in HeLa cells (Figure 4) and the level of pBAD decreases in a dose dependent way with siBAD (Figure 5), this suggests that binding to BAD is required for **1**'s apoptotic effect and that ROS are not necessarily involved in **1**'s anticancer activity. Since phosphorylation is a major regulatory mechanism by which cancer cells inhibit BAD function to suppress apoptosis, an elegant way to restore BAD activity, and thus the sensitivity of cells to apoptotic signaling without affecting the critical roles of kinases through kinase-based drugs, would be to inhibit only the phosphorylation of BAD. From our results, it is possible that this is indeed how **1** achieves its proapoptotic

activity in HeLa cells. Theoretically, **1**'s binding to BAD can either; stabilize the Bcl-xL–BAD interaction; reduce the sequestration of pBAD by 14-3-3 proteins (leaving free pBAD susceptible to phosphatases); or inhibit the phosphorylation of BAD, which favors the formation of the proapoptotic Bcl-xL–BAD complex. While our observations (Figure 1C, Figure S14) support the last mode of action, the first two possibilities remain to be refuted.

The combined effects of **1** and ABT-737, a BH3 mimic that binds to Bcl-2, Bcl-xL and Bcl-w, but not Mcl-1,⁵⁹ surprisingly revealed a highly synergistic action (Figure 6). HeLa cells are resistant to ABT-737 ($LD_{50} > 200 \mu M$), because of high levels of Mcl-1. Our results suggest that the dephosphorylation (or inhibition of phosphorylation) of BAD by **1** results in a marked increase in sensitivity of HeLa cells to ABT-737 ($LD_{50} 16 \mu M$) in the presence of $10 \mu M$ **1** and $1.2 \mu M$ with $20 \mu M$ **1**. This synergy suggests that **1** may do more than just promote the binding of BAD to Bcl-xL, and we anticipate that this target identification will enable the future exploration of many of these interesting possibilities in the clinic. Intrinsically disordered proteins (such as BAD) have the potential to bind to multiple partners depending on their conformation and post-translational modifications. Future clinical investigations of how **1** may sensitize tumors to other genotoxic agents will shed more light on the tumor selectivity of **1** and inform clinical repositioning of this fascinating natural product. Indeed, it is known that **1** synergistically induces apoptosis of HeLa cells after IR but not SiHa cells⁶⁰ and dihydroartemisinin (**5**) synergistically induces apoptosis in OVCAR-3 and A2780 (but not IOSE144) ovarian cancer cells treated with carboplatin.⁶¹ Similarly, A2780, HO8910 and HEY ovarian cancer cells responded to **1** in a dose dependent manner and are synergistic with carboplatin but SKOV3 cells were totally unresponsive to **1**.⁶² **1** has also been reported to sensitize breast cancer cells to the chemotherapeutic agent epirubicin.⁶³

Follow-up studies will include further characterization of the interaction between ART and BAD using other biophysical techniques and phosphoproteomics. The synergy between ART and AZD-59912 and S63845 (inhibitors of Mcl-1) and the interaction of ART with other BH3-only proteins will help to further characterize the cellular mechanism of ART that would not be obvious without first identifying BAD as a target of ART.

In summary, phage display is an underutilized but powerful technique for the genome wide, unbiased, reverse chemical proteomics identification of potential protein targets of small molecules. We have identified the Bcl-2 associate death promoter (BAD) as a possible human target of artesunate (**1**) in several human cancer proteomes displayed on bacteriophage T7 and shown that a possible mode of action is to interfere with BAD phosphorylation at S136. This BAD-targeting activity of **1**

is highly synergistic with the BH3 mimetic ABT-737 that binds Bcl-xL. Biophysical characterization of the interaction between ART and BAD was made difficult because BAD is an intrinsically disordered protein. Identifying and quantifying such weak and dynamic interactions is problematic and biophysical evidence usually more ambiguous than for globular proteins. However, these atypical and often weak interactions, refractory to in vivo characterization, can be very meaningful in higher-order signalling assemblies and regulation that is only now being appreciated.⁶⁴ However, overall, our data suggests a targeted mechanism of action for **1** for immediate clinical exploitation.⁵⁰

METHODS

See Supporting Information.

ASSOCIATED CONTENT

Supporting Information. Detailed synthetic procedures and probe stability, detailed target identification and validation procedures and synergistic activity data. This material is available free of charge via the internet at <http://pubs.acs.org> at DOI:

AUTHOR INFORMATION

Corresponding Author

* peter.karuso@mq.edu.au and kwonhj@yonsei.ac.kr

Present Addresses

+ Current address: School of Medical Sciences (Pharmacology), The University of Sydney, Sydney NSW 2006.

Author Contributions

‡These authors contributed equally.

Funding Sources

No competing financial interests have been declared. This work was supported by ARC grant DP130103281 to PK and HJK, NRF grant 2015K1A1A2028365, 2015M3A9C4076321 and BK21plus to HJK.

ABBREVIATIONS

BAD, Bcl-2 Antagonist of cell Death; pBAD, S136 phosphorylated BAD; siBAD, a mixture of 4 specific small interfering RNAs against BAD; ART, artesunate; F-ART, fluorescent ART.

REFERENCES

1. Mathivet, P., Bernasconi, R., Barry, J. D., Marescaux, C., and Bittiger, H. (1997) Binding characteristics of γ -hydroxybutyric acid as a weak but selective GABAB receptor agonist, *Eur. J. Pharmacol.* 321, 67–75.

2. Keilhauer, E. C., Hein, M. Y., and Mann, M. (2015) Accurate Protein Complex Retrieval by Affinity Enrichment Mass Spectrometry (AE-MS) Rather than Affinity Purification Mass Spectrometry (AP-MS), *Mol. Cell. Proteomics* 14, 120.
3. McKenzie, K. M., Videlock, E. J., Splittgerber, U., and Austin, D. J. (2004) Simultaneous Identification of Multiple Protein Targets by Using Complementary-DNA Phage Display and a Natural-Product-Mimetic Probe, *Angew. Chem. Int. Ed.* 43, 4052-4055.
4. Boehmerle, W., Splittgerber, U., Lazarus, M. B., McKenzie, K. M., Johnston, D. G., Austin, D. J., and Ehrlich, B. E. (2006) Paclitaxel induces calcium oscillations via an inositol 1,4,5-trisphosphate receptor and neuronal calcium sensor 1-dependent mechanism, *P. Natl. Acad. Sci. USA* 103, 18356-18361.
5. Izaguirre-Carbonell, J., Kawakubo, H., Murata, H., Tanabe, A., Takeuchi, T., Kusayanagi, T., Tsukuda, S., Hirakawa, T., Iwabata, K., Kanai, Y., Ohta, K., Miura, M., Sakaguchi, K., Matsunaga, S., Sahara, H., Kamisuki, S., and Sugawara, F. (2015) Novel anticancer agent, SQAP, binds to focal adhesion kinase and modulates its activity, *Sci. Rep.* 5, 15136.
6. Jung, H. J., Shim, J. S., Lee, J., Song, Y. M., Park, K. C., Choi, S. H., Kim, N. D., Yoon, J. H., Mungai, P. T., Schumacker, P. T., and Kwon, H. J. (2010) Terpestacin Inhibits Tumor Angiogenesis by Targeting UQCRB of Mitochondrial Complex III and Suppressing Hypoxia-induced Reactive Oxygen Species Production and Cellular Oxygen Sensing, *J. Biol. Chem.* 285, 11584-11595.
7. Kim, H., Deng, L., Xiong, X., Hunter, W. D., Long, M. C., and Pirrung, M. C. (2007) Glyceraldehyde 3-Phosphate Dehydrogenase Is a Cellular Target of the Insulin Mimic Demethylasterriquinone B1, *J. Med. Chem.* 50, 3423-3426.
8. Kim, N. H., Pham, N. B., Quinn, R. J., Shim, J. S., Cho, H., Cho, S. M., Park, S. W., Kim, J. H., Seok, S. H., Oh, J.-W., and Kwon, H. J. (2015) The small molecule R-(-)- β -O-methylsynephrine binds to nucleoporin 153 kDa and inhibits angiogenesis, *Int. J. Biol. Sci.* 11, 1088-1099.
9. Piggott, A. M., and Karuso, P. (2008) Rapid Identification of a Protein Binding Partner for the Marine Natural Product Kahalalide F by Using Reverse Chemical Proteomics, *ChemBioChem* 9, 524-530.
10. Piggott, A. M., Krieger, A. M., Willows, R. D., and Karuso, P. (2009) Rapid isolation of novel FK506 binding proteins from multiple organisms using gDNA and cDNA T7 phage display, *Bioorg. Med. Chem.* 17, 6841-6850.
11. Shim, J. S., Lee, J., Park, H.-J., Park, S.-J., and Kwon, H. J. (2004) A New Curcumin Derivative, HBC, Interferes with the Cell Cycle Progression of Colon Cancer Cells via Antagonization of the Ca²⁺/Calmodulin Function, *Chem. Biol.* 11, 1455-1463.
12. Woolard, J., Vousden, W., Moss, S. J., Krishnakumar, A., Gammons, M. V. R., Nowak, D. G., Dixon, N., Micklefield, J., Spannhoff, A., Bedford, M. T., Gregory, M. A., Martin, C. J., Leadlay, P. F., Zhang, M. Q., Harper, S. J., Bates, D. O., and Wilkinson, B. (2011) Borrelidin modulates the alternative splicing of VEGF in favor of anti-angiogenic isoforms, *Chem. Sci.* 2, 273-278.
13. Gotsbacher, M. P., Cho, S., Kwon, H. J., and Karuso, P. (2017) Daptomycin, a last-resort antibiotic, binds ribosomal protein S19 in humans, *Proteome Science* 15, 16.
14. Tu, Y. (2016) Artemisinin—A Gift from Traditional Chinese Medicine to the World (Nobel Lecture), *Angew. Chem. Int. Ed.* 55, in press.
15. Klayman, D. L. (1985) Qinghaosu (artemisinin): an antimalarial drug from China, *Science* 228, 1049-1055.
16. White, N. J. (2008) Qinghaosu (Artemisinin): The Price of Success, *Science* 320, 330-334.
17. O'Neill, P. M., Barton, V. E., and Ward, S. A. (2010) The molecular mechanism of action of artemisinin - the debate continues, *Molecules* 15, 1705-1721.
18. Stocks, P. A., Bray, P. G., Barton, V. E., Al-Helal, M., Jones, M., Araujo, N. C., Gibbons, P., Ward, S. A., Hughes, R. H., Biagini, G. A., Davies, J., Amewu, R., Mercer, A. E., Ellis, G., and O'Neill, P. M. (2007) Evidence for a Common Non-Heme Chelatable-Iron-Dependent Activation Mechanism for Semisynthetic and Synthetic Endoperoxide Antimalarial Drugs, *Angew. Chem. Int. Ed.* 46, 6278-6283.
19. Ismail, H. M., Barton, V. E., Panchana, M., Charoensuthivarakul, S., Biagini, G. A., Ward, S. A., and O'Neill, P. M. (2016) A Click Chemistry-Based Proteomic Approach Reveals that 1,2,4-Trioxolane and Artemisinin Antimalarials Share a Common Protein Alkylation Profile, *Angew. Chem. Int. Ed.* 55, 6401-6405.
20. Robert, A., Cazelles, J., and Meunier, B. (2001) Characterization of the Alkylation Product of Heme by the Antimalarial Drug Artemisinin, *Angew. Chem. Int. Ed.* 40, 1954-1957.
21. Wang, J., Zhang, C.-J., Chia, W. N., Loh, C. C. Y., Li, Z., Lee, Y. M., He, Y., Yuan, L.-X., Lim, T. K., Liu, M., Liew, C. X., Lee, Y. Q., Zhang, J., Lu, N., Lim, C. T., Hua, Z.-C., Liu, B., Shen, H.-M., Tan, K. S. W., and Lin, Q. (2015) Haem-activated promiscuous targeting of artemisinin in Plasmodium falciparum, *Nat. Comm.* 6, 10111.
22. Eckstein-Ludwig, U., Webb, R. J., van Goethem, I. D. A., East, J. M., Lee, A. G., Kimura, M., O'Neill, P. M., Bray, P. G., Ward, S. A., and Krishna, S. (2003) Artemisinins target the SERCA of Plasmodium falciparum, *Nature* 424, 957-961.
23. Lisewski, A. M., Quiros, J. P., Ng, C. L., Adikesavan, A. K., Miura, K., Putluri, N., Eastman, R. T., Scanfeld, D., Regenbogen, S. J., Altenhofen, L., Llinas, M., Sreekumar, A., Long, C., Fidock, D. A., and Lichtarge, O. (2014) Supergenomic network compression and the discovery of EXP1 as a glutathione transferase inhibited by artesunate, *Cell* 158, 916-928.
24. Mbengue, A., Bhattacharjee, S., Pandharkar, T., Liu, H., Estiu, G., Stahelin, R. V., Rizk, S. S., Njimoh, D. L., Ryan, Y., Chotivanich, K., Nguon, C., Ghorbal, M., Lopez-Rubio, J. J., Pfreder, M., Emrich, S., Mohandas, N., Dondorp, A. M., Wiest, O., and Haldar, K. (2015) A molecular mechanism of artemisinin resistance in Plasmodium falciparum malaria, *Nature* 520, 683-687.
25. Efferth, T., Dunstan, H., Sauerbrey, A., Miyachi, H., and Chitambar, C. R. (2001) The anti-malarial artesunate is also active against cancer, *Int. J. Oncol.* 18, 767-773.
26. Singh, N. P., and Lai, H. C. (2004) Artemisinin induces apoptosis in human cancer cells, *Anticancer Res.* 24, 2277-2280.
27. Efferth, T. (2006) Molecular pharmacology and pharmacogenomics of artemisinin and its derivatives in cancer cells, *Curr. Drug Targets* 7, 407-421.
28. Ho, W. E., Peh, H. Y., Chan, T. K., and Wong, W. S. F. (2014) Artemisinins: Pharmacological actions beyond anti-malarial, *Pharmacol. Ther.* 142, 126-139.
29. Lai, H. C., Singh, N. P., and Sasaki, T. (2013) Development of artemisinin compounds for cancer treatment, *Invest. New Drugs* 31, 230-246.
30. Kwok, J. C., and Richardson, D. R. (2002) The iron metabolism of neoplastic cells: alterations that facilitate proliferation?, *Crit. Rev. Oncol. Hematol.* 42, 65-78.

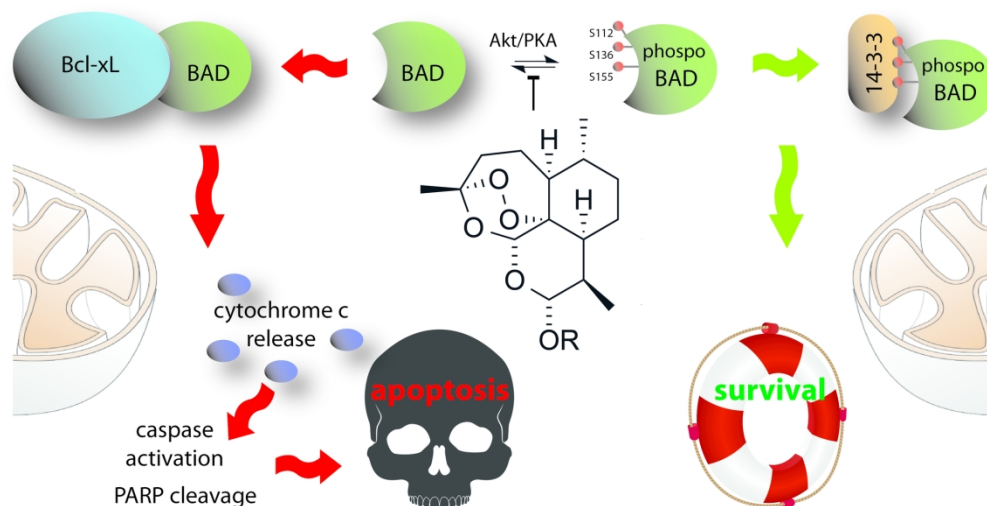
31. Efferth, T. (2007) Willmar Schwabe Award 2006: antiparasitic and antitumor activity of artemisinin - from bench to bedside, *Planta Med.* 73, 299-309.
32. Huang, C., Ba, Q., Yue, Q., Li, J., Li, J., Chu, R., and Wang, H. (2013) Artemisinin rewires the protein interaction network in cancer cells: network analysis, pathway identification, and target prediction, *Mol. BioSyst.* 9, 3091-3100.
33. Odaka, Y., Xu, B., Luo, Y., Shen, T., Shang, C., Wu, Y., Zhou, H., and Huang, S. (2014) Dihydroartemisinin inhibits the mammalian target of rapamycin-mediated signaling pathways in tumor cells, *Carcinogenesis* 35, 192-200.
34. Thanaketaipaisarn, O., Waiwut, P., Sakurai, H., and Saiki, I. (2011) Artesunate enhances TRAIL-induced apoptosis in human cervical carcinoma cells through inhibition of the NF- κ B and PI3K/Akt signaling pathways, *Int. J. Oncol.* 39, 279-285.
35. Cho, S., Oh, S., Um, Y., Jung, J.-H., Ham, J., Shin, W.-S., and Lee, S. (2009) Synthesis of 10-substituted triazolyl artemisinins possessing anticancer activity via Huisgen 1,3-dipolar cycloaddition, *Bioorg. Med. Chem. Lett.* 19, 382-385.
36. Hinds, M. G., Smits, C., Fredericks-Short, R., Risk, J. M., Bailey, M., Huang, D. C., and Day, C. L. (2007) Bim, Bad and Bmf: intrinsically unstructured BH3-only proteins that undergo a localized conformational change upon binding to prosurvival Bcl-2 targets, *Cell Death Differ.* 14, 128-136.
37. Yang, E., Zha, J., Jockel, J., Boise, L. H., Thompson, C. B., and Korsmeyer, S. J. (1995) Bad, a heterodimeric partner for Bcl-xL and Bcl-2, displaces bax and promotes cell death, *Cell* 80, 285-291.
38. Lomenick, B., Hao, R., Jonai, N., Chin, R. M., Aghajani, M., Warburton, S., Wang, J., Wu, R. P., Gomez, F., Loo, J. A., Wohlschlegel, J. A., Vondriska, T. M., Pelletier, J., Herschman, H. R., Clardy, J., Clarke, C. F., and Huang, J. (2009) Target identification using drug affinity responsive target stability (DARTS), *P. Natl. Acad. Sci. USA* 106, 21984-21989.
39. Pommier, Y. (2006) Topoisomerase I inhibitors: camptothecins and beyond, *Nat. Rev. Cancer* 6, 789-802.
40. Efferth, T. (2014) Activation of Mitochondria-Driven Pathways by Artemisinin and Its Derivatives, In *Mitochondria: The Anti-cancer Target for the Third Millennium* (Neuzil, J., Pervaiz, S., and Fulda, S., Eds.), pp 135-150, Springer Netherlands.
41. Tran, K. Q., Tin, A. S., and Firestone, G. L. (2014) Artemisinin triggers a G1 cell cycle arrest of human Ishikawa endometrial cancer cells and inhibits cyclin-dependent kinase-4 promoter activity and expression by disrupting nuclear factor- κ B transcriptional signaling, *Anticancer Drugs* 25, 270-281.
42. Efferth, T., Sauerbrey, A., Olbrich, A., Gebhart, E., Rauch, P., Weber, H. O., Hengstler, J. G., Halatsch, M.-E., Volm, M., Tew, K. D., Ross, D. D., and Funk, J. O. (2003) Molecular modes of action of artesunate in tumor cell lines, *Mol. Pharmacol.* 64, 382-394.
43. Button, R. W., Lin, F., Ercolano, E., Vincent, J. H., Hu, B., Hanemann, C. O., and Luo, S. (2014) Artesunate induces necrotic cell death in schwannoma cells, *Cell Death Dis.* 5, e1466.
44. Ooko, E., Saeed, M. E. M., Kadioglu, O., Sarvi, S., Colak, M., Elmasaoudi, K., Janah, R., Greten, H. J., and Efferth, T. (2015) Artemisinin derivatives induce iron-dependent cell death (ferroptosis) in tumor cells, *Phytomedicine* 22, 1045-1054.
45. Zhou, Y., Li, W., and Xiao, Y. (2016) Profiling of Multiple Targets of Artemisinin Activated by Hemin in Cancer Cell Proteome, *ACS Chem. Biol.*
- independent and Bax-mediated intrinsic pathway in HepG2 cells, *Exp. Cell Res.* 336, 308-317.
47. Zhang, F., Gosser, D. K., and Meshnick, S. R. (1992) Hemin-catalyzed decomposition of artemisinin (qinghaosu), *Biochem. Pharmacol.* 43, 1805-1809.
48. Czabotar, P. E., Lessene, G., Strasser, A., and Adams, J. M. (2014) Control of apoptosis by the BCL-2 protein family: implications for physiology and therapy, *Nat. Rev. Mol. Cell Biol.* 15, 49-63.
49. Adams, J. M., and Cory, S. (2007) The Bcl-2 apoptotic switch in cancer development and therapy, *Oncogene* 26, 1324-1337.
50. Crespo-Ortiz, M. P., and Wei, M. Q. (2012) Antitumor activity of artemisinin and its derivatives: from a well-known antimalarial agent to a potential anticancer drug, *J. Biomed. Biotechnol.* 2012, 247597.
51. Leo, C. P., Hsu, S. Y., Chun, S. Y., Bae, H. W., and Hsueh, A. J. (1999) Characterization of the antiapoptotic Bcl-2 family member myeloid cell leukemia-1 (Mcl-1) and the stimulation of its message by gonadotropins in the rat ovary, *Endocrinology* 140, 5469-5477.
52. Danial, N. N., and Korsmeyer, S. J. (2004) Cell death: critical control points, *Cell* 116, 205-219.
53. She, Q. B., Solit, D. B., Ye, Q., O'Reilly, K. E., Lobo, J., and Rosen, N. (2005) The BAD protein integrates survival signaling by EGFR/MAPK and PI3K/Akt kinase pathways in PTEN-deficient tumor cells, *Cancer cell* 8, 287-297.
54. Andreeff, M., Jiang, S., Zhang, X., Konopleva, M., Estrov, Z., Snell, V. E., Xie, Z., Okcu, M. F., Sanchez-Williams, G., Dong, J., Estey, E. H., Champlin, R. C., Kornblau, S. M., Reed, J. C., and Zhao, S. (1999) Expression of Bcl-2-related genes in normal and AML progenitors: changes induced by chemotherapy and retinoic acid, *Leukemia* 13, 1881-1892.
55. Datta, S. R., Dudek, H., Tao, X., Masters, S., Fu, H., Gotoh, Y., and Greenberg, M. E. (1997) Akt phosphorylation of BAD couples survival signals to the cell-intrinsic death machinery, *Cell* 91, 231-241.
56. del Peso, L., Gonzalez-Garcia, M., Page, C., Herrera, R., and Nunez, G. (1997) Interleukin-3-induced phosphorylation of BAD through the protein kinase Akt, *Science* 278, 687-689.
57. Donovan, N., Becker, E. B., Konishi, Y., and Bonni, A. (2002) JNK phosphorylation and activation of BAD couples the stress-activated signaling pathway to the cell death machinery, *J. Biol. Chem.* 277, 40944-40949.
58. Zha, J., Harada, H., Yang, E., Jockel, J., and Korsmeyer, S. J. (1996) Serine phosphorylation of death agonist BAD in response to survival factor results in binding to 14-3-3 not Bcl-x(L), *Cell* 87, 619-628.
59. Oltersdorf, T., Elmore, S. W., Shoemaker, A. R., Armstrong, R. C., Augeri, D. J., Belli, B. A., Bruncko, M., Deckwerth, T. L., Dinges, J., Hajduk, P. J., Joseph, M. K., Kitada, S., Korsmeyer, S. J., Kunzer, A. R., Letai, A., Li, C., Mitten, M. J., Nettesheim, D. G., Ng, S. C., Nimmer, P. M., O'Connor, J. M., Oleksijew, A., Petros, A. M., Reed, J. C., Shen, W., Tahir, S. K., Thompson, C. B., Tomaselli, K. J., Wang, B., Wendt, M. D., Zhang, H., Fesik, S. W., and Rosenberg, S. H. (2005) An inhibitor of Bcl-2 family proteins induces regression of solid tumours, *Nature* 435, 677-681.
60. Luo, J., Zhu, W., Tang, Y., Cao, H., Zhou, Y., Ji, R., Zhou, X., Lu, Z., Yang, H., Zhang, S., and Cao, J. (2014) Artemisinin derivative artesunate induces radiosensitivity in cervical cancer cells in vitro and in vivo, *Radiat. Oncol.* 9, 84.

61. Chen, T., Li, M., Zhang, R., and Wang, H. (2009) Dihydroartemisinin induces apoptosis and sensitizes human ovarian cancer cells to carboplatin therapy, *J. Cell. Mol. Med.* *13*, 1358-1370.

62. Wang, B., Hou, D., Liu, Q., Wu, T., Guo, H., Zhang, X., Zou, Y., Liu, Z., Liu, J., Wei, J., Gong, Y., and Shao, C. (2015) Artesunate sensitizes ovarian cancer cells to cisplatin by downregulating RAD51, *Cancer Biol. Ther.* *16*, 1548-1556.

63. Chen, K., Shou, L.-M., Lin, F., Duan, W.-M., Wu, M.-Y., Xie, X., Xie, Y.-F., Li, W., and Tao, M. (2014) Artesunate induces G2/M cell cycle arrest through autophagy induction in breast cancer cells, *Anticancer Drugs* *25*, 652-662.

64. Berlow, R. B., Dyson, H. J., and Wright, P. E. (2018) Expanding the Paradigm: Intrinsically Disordered Proteins and Allosteric Regulation, *J. Mol. Biol.* *430*, 2309-2320.



The antimalarial artesunate targets BAD in the Bcl-xL proapoptotic pathway in humans

177x91mm (300 x 300 DPI)